Ab Initio Molecular Dynamics Simulation of a Room Temperature Ionic Liquid

Mario G. Del Pópolo,[†] Ruth M. Lynden-Bell,[‡] and Jorge Kohanoff*[,†]

Atomistic Simulation Centre, School of Mathematics and Physics, Queen's University Belfast, Belfast BT7 1NN, U.K., and University Chemical Laboratory, Lensfield Road, Cambridge University, Cambridge CB2 1EW, U.K.

Received: December 8, 2004

Ab initio molecular dynamics simulations have been performed for the first time on the room-temperature organic ionic liquid dimethyl imidazolium chloride [DMIM][Cl] using density functional theory. The aim is to compare the local liquid structure with both that obtained from two different classical force fields and from neutron scattering experiments. The local structure around the cation shows significant differences compared to both the classical calculations and the neutron results. In particular, and unlike in the gas-phase ion pair, chloride ions tend to be located near a ring C−H proton in a position suggesting hydrogen bonding. The results are used to suggest ways in which the classical potentials may be improved.

1. Introduction

Room temperature molten salts, or Ionic Liquids, are liquids formed solely of ions. Unlike inorganic molten salts such as NaCl, they are fluid at room temperature, or at least within the typical temperature range of most organic chemical reactions.[1,2] Ionic Liquids possess appealing features that make them attractive in different areas of chemistry; for example, they exhibit an almost vanishing vapor pressure, the characteristic electrical conductivity of an ionic conductor, and a considerable gap between the melting point and the temperature of decomposition.[1] The possibility of driving the course of chemical reactions, added to an ubiquitous low vapor pressure, makes these fluids an attractive alternative to traditional organic solvents for both laboratory and industrial purposes.

Because of this interest several fundamental aspects of Ionic Liquids have been studied in the past few years, both experimentally and computationally. In the first class, it is worth mentioning experiments of solute rotation and solvation dynamics,[3] reorientational dynamics using Kerr spectroscopy,[4] relaxation dynamics by means of quasielastic neutron scattering,[5] Raman band shape analysis,[6] hydrogen bonding[7] and ionic mobilities and liquid fragilities.[8] Of particular relevance for the present work are neutron diffraction studies of a few model Ionic Liquids.[9,10]

Many computer simulations on different model systems have also been reported. Some work has been devoted to the development of classical[11−16] and even polarizable force fields.[17] Simulations have concerned thermodynamic,[18,19] structural[11,20] and dynamical properties[15,20] of both pure Ionic Liquids and mixtures with simple solutes.[21] The only previous ab initio studies concern different isolated ion pairs in a vacuum.[22]

2. Motivations for an ab Initio Study

The structure of Ionic Liquids, as is the case of any fluid formed purely of ions, results from a competition between screening and packing. This means a balance between long-range electrostatic forces and geometric factors associated with the shape of the molecules. Organic molten salts have asymmetric and diffusely charged cations; these properties frustrate the easy packing of the ions and increase the fluidity of the material.

Whereas the local density of a nonassociating fluid can be relatively insensitive to the details of the intermolecular interactions, in Ionic Liquids the distribution of counterions around certain chemical bonds strongly depends on such details. Site−site radial distribution functions and three-dimensional densities are good descriptors of the solvation structure of the ions. These functions are expected to exhibit important changes in going from classical to quantum models, where polarization and charge-transfer effects occur naturally.

1,3-Dimethylimidazolium chloride ([DMIM][Cl]) is one of the simplest Ionic Liquids. Its structure has been studied by neutron scattering experiments, and some differences in the spatial distribution of chloride ions about the cation compared to those from classical simulations were found.[9,10] The source of these differences is not clear yet. On one hand, experiments do not provide direct information about the full angular-dependent partial density functions. Such dependence has to be obtained by means of a refinement procedure (EPRS) that generates correlation functions compatible with the measured structure factors.[23,24] Such distribution functions are however not completely free of ambiguity. On the other hand, the electrostatic models used for classical simulations have been parametrized from the cation properties in the gas phase.[11−16] However it is a well-known fact that the effective dipole moment in the liquid state may differ from that in the gas phase, for example, nonpolarizable models of liquid water have significantly higher dipole moments than does the isolated molecule.

The classical force fields used so far are based on site−site terms. Most of them have fixed partial charges and either Buckingham or Lennard-Jones interaction centers on the atomic sites. These have been parametrized using a combination of standard values for the repulsive part of the potential and gas-phase ab initio calculations to determine the partial charges.[11−16] In general, the level of agreement between the known experi-

* Corresponding author. Tel: ++44 (2890) 973770; Fax: ++44 (2890) 975359; E-mail: j.kohanoff@qub.ac.uk.
[†] Queen's University Belfast.
[‡] Cambridge University.

10.1021/jp044414g CCC: $30.25
Published on Web 03/02/2005

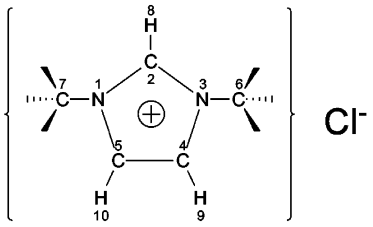

Figure 1. Dimethylimidazolium chloride ([DMIM][Cl]).

mental structures and that obtained from classical simulations is acceptable. However, there are discrepancies between different models and between models and experiment. In particular, some structural features such as anion-hydrogen distributions are affected by directional interactions that would involve some degree of local polarization or even charge transfer between molecules.

The aim of the present work is to study, by means of ab initio molecular dynamics simulations, the structure of the Ionic Liquid 1,3-dimethylimidazolium chloride [DMIM][Cl], whose molecular formula is shown in Figure 1. The results will be compared to previously reported classical simulations and to neutron scattering experiments with the aim of pinpointing shortcomings in the classical potentials. This paper is organized as follows: computational methods and technical details are described in Section 3. Results on the structure of different phases of [DMIM][Cl], as well as hydrogen bonding, are presented in Section 4. In Section 5 we summarize the most important conclusions.

3. Computational Methods

We have performed Density functional-based, molecular dynamics simulations using the SIESTA program.[25] SIESTA is an electronic structure code where core electrons are replaced by norm-conserving pseudopotentials, and the electronic orbitals are expanded in a nonorthogonal basis set of atom-centered orbitals. These orbitals are the solution of the pseudoatomic problem, with the additional condition that they exactly vanish at a finite cutoff radius. This condition results in an energy shift of the eigenvalues with respect to the isolated pseudoatoms (infinite radius). We have chosen an energy shift of 50 meV, which proved to be sufficiently small for the convergence of structural and energetic properties. The electrostatic and exchange-correlation interactions are calculated using a real-space grid approach and Fast Fourier Transforms. The spacing of the grid points chosen corresponds to an equivalent energy cutoff of 200 Ry in the associated reciprocal space. Again, structural and electronic properties have converged at this value. For the exchange-correlation term of the energy functional we used the generalized gradient approximation (GGA) proposed by Perdew, Burke and Ernzerhof,[26] which proved quite accurate in a number of different situations, including gas and condensed phases, and hydrogen-bonded systems. The pseudopotentials have been generated according to the prescription of Troullier and Martins.[27] The basis set was tested in the solid phase, against fully converged plane wave calculations using the same pseudopotentials and the CPMD code.[28] All calculations of the liquid state use periodic boundary conditions in order to model bulk behavior with a limited number of molecules.

Two different model systems were studied for the liquid phase. The first consisted of 8 ion pairs (136 atoms) in a cubic box of side 11.6 Å, which provided the most significant results of this paper. The second was a significantly larger system consisting of 24 ion pairs (408 atoms) in a dodecahedral (*fcc*) box. The smallest system represented a good compromise between system dimensions and the time scale accessible to a single trajectory. The second system was used mainly as a test for convergence with system size. The density of the liquid was always set to the experimental value of 0.087 atoms/Å^3 at a temperature of 425 K.[29] The gas phase was modeled by a single ion pair in a cubic box of 20 Å side, for a total integration time of 12 ps.

Since structural properties are independent of the mass of the particles, hydrogen atoms were replaced by deuterium. This allowed us to use larger time steps, 0.75 fs in the present case, without compromising energy conservation. For the 8 ion pairs system, six trajectories of 6−7 ps were generated, representing a total simulation time of approximately 39 ps, excluding equilibration periods of 1.5 ps per trajectory. For the largest system, only one trajectory of 3.5 ps was considered. All the calculations were carried out in a cluster of PCs running on Opteron CPUs, in a parallel architecture.

It is well-known that the dynamics of Ionic Liquids is slow.[15,20] Therefore, a legitimate point of concern is the effect of the limited simulation time on the various structural properties. To circumscribe such effects a systematic procedure was followed. Two sets of initial configurations were generated from classical simulations, using two well-established force fields.[11,16] Each of these simulations was started from a different random structure and was equilibrated for more than 6 ns at 450 K; the final states were then considered independent. These configurations were the starting points of the six ab initio simulations.

The site−site radial distribution functions calculated during the classical runs are somewhat different for the two classical models. The two sets of ab initio trajectories were then subjected to a convergence test. At the end of the ab initio simulations, the cation−anion distributions calculated from the first set of trajectories were the same (within the error bars) as the ones calculated from the second set starting from the second classical model. In addition, the ab initio distribution functions were different from the classical ones, showing independence from the initial configurations. We are thus confident of the statistical significance of the present results.

The reason cation−anion space-correlation functions converged within the time scales considered in this work is because the correction imposed by the ab initio approach on the initial classical configuration does not involve a dramatic structural rearrangement. Changes in the first solvation shell of a cation are mostly restricted to a rearrangement of the positions of the anions, and no cage breaking is required. If this last process were required, then times far beyond the current capabilities of ab initio simulations would be necessary.

On the basis of the above considerations, it must be emphasized that the structure of the first solvation shell of the cation represents the most significant results of this paper. There are two reasons for that, system size effects and sampling difficulties. While in the smallest system the sampling was appropriate, the half-cell length is barely as large as the position of the first peak of the anion−anion and cation−cation distributions as inferred from experimental information and classical simulations. Finite size effects are then expected to affect those distributions. In the largest system, size effects are mitigated, but a single trajectory of 3.5 ps is not enough for the cations to sample different orientations. However, it appears that cation−anion contacts are remarkably independent of the system size, most likely due to the importance of short-range forces. Long-range forces are effectively screened out in the ionic environment.

TABLE 1: Intermolecular Contacts and Intramolecular Parameters for the Solid Phase of [DMIM][Cl], Calculated Using SIESTA and Plane Waves (CPMD), as Compared with the X-ray Structure (EXP.)[30a]

	$Cl^-\cdots Cl^-$	$Cl^-\cdots H_8$	$Cl^-\cdots H_{9,10}$	C_2-H_8	$C_{4,5}-H_{9,10}$	$N-C_2-H_8$	C_2-N-C_{met}
SIESTA	4.31	2.57	2.43	1.11	1.11	124.2, 127.6	124.8, 125.7
CPMD	4.31	2.58	2.46	1.10	1.10	124.3, 127.5	124.8, 125.8
EXP.	4.64	2.56	2.59	1.08	1.08	125.1, 126.5	125.2, 126.1

[a] $Cl^-\cdots X$ represents different intermolecular contacts (in Å) that involve the anion. C−H bond lengths, are also reported in Å, and the atom labels correspond to those of Figure 1. Some representative bond angles are shown in the last two columns. Two of these angles are present per cation and are slightly different between themselves in the solid phase.

4. Results and Discussion

4.1. Structure of the Solid Phase. The crystal structure of [DMIM][Cl] has been determined experimentally.[30] To test the performance of our ab initio approach, the optimized structure of the solid was compared both with an equivalent plane wave calculation (which is more accurate, but much slower) and with the experimental X-ray structure. Nuclei were allowed to relax starting from the experimental structure within a unit cell constrained to the experimental size and shape.

Table 1 shows some intermolecular distances and intramolecular parameters for the two ab initio calculations and the X-ray crystal structure. Only those quantities that deviate most from the experiment are shown. The intramolecular structure of the $[DMIM]^+$ ion is consistently well described by the two theoretical methods. Intermolecular distances differ more from the experimental structure, due to a small rotation of both the cation planes and the methyl groups. The absolute deviation in the position of Cl^-, between SIESTA and the experiment, was 0.17 Å, whereas between the two calculations it was 0.004 Å.

By relaxing also the cell parameters we found a reasonable agreement with experiment but not to the extent shown by the internal geometry. The quality of the lattice parameters from the plane wave calculations was not significantly better than that obtained with SIESTA. Therefore the disagreement has to be attributed to the energy functional. Present day density functionals are not accurate enough to systematically reproduce lattice parameters to an accuracy better than a few percent. In the present case, the problem is likely to be due to the dispersion interactions, which are not fully taken into account within GGA. In cases such as this, where the unit cell is monoclinic, the angle may be quite sensitive to the functional.

In general terms it is clear that the solid structure given by SIESTA is much closer to that obtained with plane waves than to the experimental one. This is an important test for the type of calculations used in this paper. It allows us to attribute the differences from experiment to either a limitation of the exchange-correlation functional or to limitations in the accuracy of the X-ray structure (or both).

4.2. The Isolated Ion Pair. Simulations of the isolated ion pair at 450 K served as a reference to calculate the internal energy of the liquid and helped to identify some effects that appear only in the condensed phases. This model may not represent a real vapor of [DMIM][Cl] where clustering of several ionic pairs could be present. However, in the rest of this paper we will refer to these simulations as the 'gas phase'.

As a first step, the geometry of the isolated ion pair was optimized starting from two different initial configurations. These resulted in the minimum energy structures shown in Figure 2, where some interatomic distances and angles have been included. Configuration a) was found to be 0.14 eV more stable than structure b), i.e., about 3.6 kT at the temperature of the simulations described below.

In case a) the chloride ion is localized above the plane of the imidazolium, practically on top of the unique carbon, C_2. A detail to notice is the departure of the ring from planarity, concomitant with the pyramidal pattern shown by C_2. In the second isomer the anion finds a local minimum in the plane of the ring, where it can interact with the unique hydrogen H_8 and the methyl hydrogens. These results agree with the earlier work of Turner et al.[22] In addition, there are other similar local minima where the anion is localized close to H_4 and H_5.

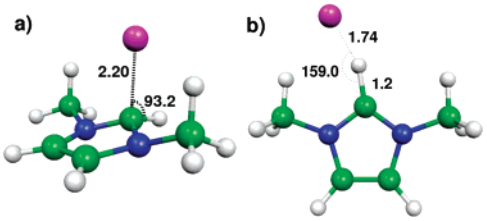

Figure 2. Minimum energy configurations of an isolated ion pair of [DMIM][Cl]. Some distances (in Å) and angles between the anion and cation atoms are shown.

In a second stage, the effects of temperature were included by means of AIMD simulations started from the two optimized structures. Chlorides rattled around the minimum energy configurations of Figure 2, while the cation exhibited significant fluctuations in its geometry. During the course of several picoseconds no transitions were observed between the two minima indicating that they are separated by an energy barrier higher than the thermal energy at 450 K. For the simulation started from a) the anion remained localized above the axis of the C_2-H_8 bond. Therefore, the probability of finding the anion in a position collinear with any of the C−H bonds was negligible, and no directional $H\cdots Cl^-$ contacts were observed. For the second simulation the anion remained on the perimeter of the ring forming an angle of around 160° with the C_2-H_8 bond. This indicates that the interaction between chloride and ring-hydrogens is already directional in the gas phase, although at the temperature of interest here the population of configuration b) is much lower than a). For this reason the following discussion will be restricted to the simulation around the global minimum.

Distribution functions of bond lengths, bending and dihedral angles that exhibited the largest differences between the gas and the liquid phase are shown in Figure 3. The $N_{1,3}-C_2$ bond length distribution is broader and shifted toward longer distances in the isolated pair, while the one for C_2-H_8 is broader in the liquid. The bond angle distributions that are most affected involved the unique carbon and the methyl groups. Finally, dihedral distributions show that the methyl groups move from the bent structure of Figure 2 to being in the plane of the ring in the liquid, more like for isomer b) in Figure 2. In general, all those changes in the intramolecular structure are related to a significant change in the optimum relative position of the ions between the two phases. As will be shown below, in the liquid, anions are located on the perimeter of the cation, and configurations derived from metastable isomers in the gas phase, like b) in Figure 2, appear to be favored in the condensed phases. There, each ion is surrounded by several counterions, and the intra-

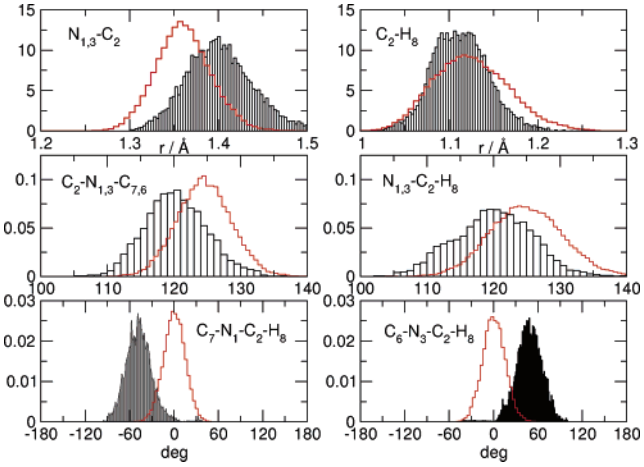

Figure 3. Distribution functions for the intramolecular parameters of $[DMIM]^+$ that showed the largest variation between the gas and the liquid phase. In the upper panels are shown the bond-length distributions, while middle and lower panels correspond to bond-angle and dihedral distributions. In all the plots, histograms without vertical lines correspond to the liquid phase. Atom labels are shown in Figure 1.

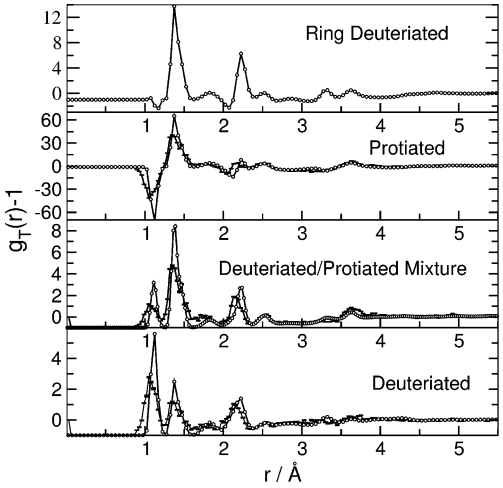

Figure 4. Neutron weighted total radial distribution functions $g_T(r) - 1$, for different H-isotopic substitutions of [DMIM][Cl]. The same substitutions reported in Figure 3 of ref 9 are shown. Solid lines with circles and dashed lines with error bars correpond to calculated and experimental curves, respectively.

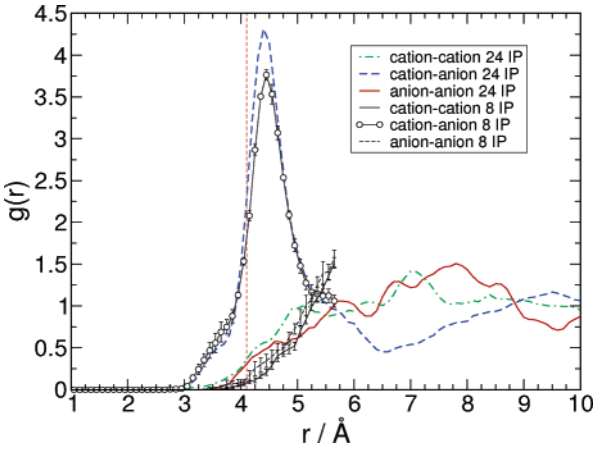

Figure 5. Radial distribution functions (RDFs) calculated from the geometric center of the cations. Lines with error bars correspond to the ab initio simulations with 8 ion pairs. Error bars were calculated by averaging over six different simulations. RDFs expanding up to 10 Å correspond to the ab initio simulation with 24 ion pairs. The vertical line indicates the cation−anion distance in the solid phase. These functions are provided as Supporting Information.

molecular structure of $[DMIM]^+$ is affected by the structure of its first solvation shell.

4.3. Liquid Structure. A distinctive feature of molten salts is their low vapor pressure. This is mainly due to the long-range electrostatic interactions that confer a high energy density to the material. For [DMIM][Cl], we estimated a cohesive energy of 1.6 eV (155 kJ/mol) per formula unit. This was obtained as the difference between the average DFT energies of the gas and the liquid phase at 450 K. Such cohesive energy is similar to that of inorganic molten salts (184 kJ/mol for AgCl and 114 kJ/mol for $CdCl_2$ at the boiling points) but quite high compared with non-Ionic Liquids (41.5 kJ/mol for water at 298 K and 27.5 kJ/mol for cyclohexane at the boiling point) and even with electrolytic solutions, where the dielectric screening of the solvent results in weaker effective interactions between the ions. This energetic behavior is also accompanied by peculiar structural properties.

The local structure of molten salts is the result of a delicate balance between packing and screening. The first effect is dependent on the shape of the molecules, while the second arises from the slowly decaying electrostatic interactions. The screening mechanism determines the long-range behavior of the ionic distribution functions and leads to charge ordering effects at low temperatures,[31] normally an alternation in the sign of the charge associated with successive solvation layers around the ions. Radial distribution functions of particles of the same charge and particles of different charges exhibit out-of-phase oscillations slowly decaying with distance.

Neutron diffraction experiments provide valuable information on the structure of fluids. Unfortunately, for molecular liquids this information is restricted to a few total radial distribution functions, $g_T(r)$, according to the number of isotopic substitutions performed. Each $g_T(r)$ is given by a weighted sum of all the possible atom−atom radial distributions, and the weight depends on the isotopic nature of the atoms involved in the pair.[31] To compare the simulation results with the information provided directly by the experiment, Figure 4 shows various theoretical neutron weighted $g_T(r)$ together with their experimental counterparts, for various isotopic substitutions.[9] It is clear that almost all of the features are observed at distances lower than the effective radius of the cation (∼3.0 Å). In addition, by switching off all the intermolecular contributions the calculated functions remain practically unchanged, indicating that almost all the scattering is intramolecular. Theoretical and experimental curves in Figure 4 are very similar; the information about intermolecular structure lies in small details near the baseline.

In contrast to most inorganic molten salts, room temperature Ionic Liquids are complex molecular fluids. The effective electrostatic interaction is angular-dependent, and the microscopic structure cannot be fully described by intermolecular radial distribution functions. However, apart from directionality issues, charge ordering effects are readily seen in radial functions measured from the center of the ions. Figure 5 shows such functions for [DMIM][Cl] at 450 K, calculated for the two systems described in section 3, with 8 and 24 ion pairs, respectively. The position of the first peak in the distribution of anions, at 4.5 Å, is size-independent and slightly larger than the corresponding distance in the solid (4.2 Å, vertical dashed line in Figure 5). The position and height of this first peak correspond very well with the experimental value,[9] although certain differences between the two ab initio system sizes are observed. These can be attributed to the lack of statistics in the

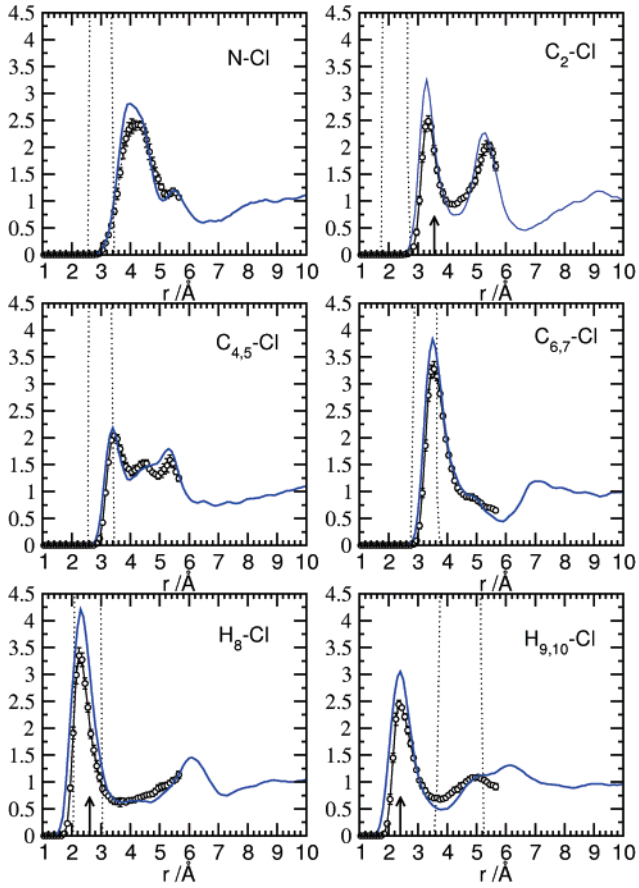

Figure 6. Site−site radial distribution functions, $g_{ab}(r)$, between different cation atoms and chloride. Lines with circles and solid lines correspond to the systems with 8 and 24 ion-pairs, respectively. The corresponding distributions for the isolated ionic pair at 450 K are localized between the two vertical dotted lines. Arrows represent the contacts in the solid phase. Atom labels are shown in Figure 1. These functions are provided as Supporting Information.

system of 24 ions. Each imidazolium is surrounded by 6 anions up to a distance of 6.5 Å. Cation−cation and anion−anion distributions are reported in Figure 5 just for completeness; these clearly show the presence of charge ordering effects.

Classical simulations, where different dispersive and electrostatic models were used, led to quite similar results for the radial distributions defined from the center of the ions. From ref 17 it is clear that even the inclusion of polarizabilities in the force field does not affect too much the center-of-mass cation−anion distributions with respect to the nonpolarizable case.

Site−site radial distribution functions between individual cation atoms and the chloride ion contain valuable information about the local environment of each functional group. Classical simulations indicate that they are quite sensitive to the details of the intermolecular forces. Figure 6 shows site−site distributions calculated for the two ab initio systems. Again, the position of the peaks is size-independent, but the amplitudes are slightly different. The H_8−Cl and $H_{9,10}$−Cl distributions deserve to be discussed in detail, because they differ from the results of both experiments and classical simulations. Both functions show a first sharp peak at 2.2 Å and a second broader maximum at approximately 6.0 Å. This second peak is associated with the anions located in the proximity of the other ring-hydrogens, some of them on the opposite side of the cation. The coordination number of H_8 and $H_{9,10}$ is 1, up to a distance of 3.5 Å, and, as will be discussed later, these chlorides seem to be highly localized in the neighborhood of the hydrogens. A similar

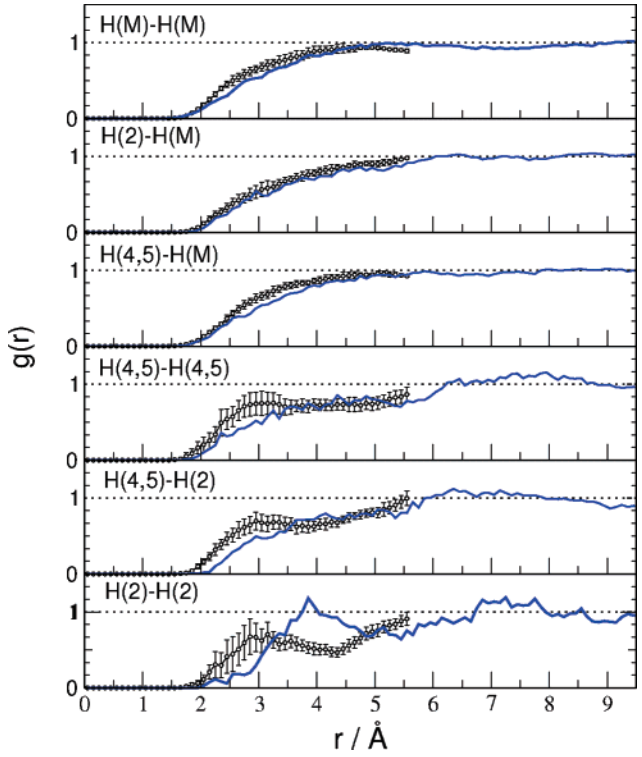

Figure 7. Site−site pair distribution functions for intermolecular hydrogen distances. Lines with circles and solid lines correspond to the simulations with 8 and 24 ion pairs, respectively. Error bars calculated from six independent simulations. Atom labels are detailed in Figure 1. Functions provided as Supporting Information.

analysis of the Cl−H_{Met} (methyl-hydrogens) distributions gave two broad maxima, one at 2.5 Å, which is similar to the corresponding distance in the solid, and another at 4.4 Å.

To see how the structure of the first solvation layer of [DMIM][Cl] changes between the different phases, we have also included in Figure 6 information about the isolated ion par and the solid. For the gas phase we have only considered the simulation corresponding to the most stable minimum. The dotted vertical lines indicate the position and width of the maximum in the ion-pair site−site distributions. The arrows indicate the corresponding distances in the solid. Clearly the shortest contacts are very similar between liquid and solid, apart from the broadening and a small shift. The probability distributions, however, change importantly when going from the most stable structure in the gas phase to the condensed phase. These structural changes are to be expected because in the isolated ion pair, Cl^- is basically localized above the imidazolium plane, where it is close to the unique carbon C_2 (see Figure 2). In this configuration the anion interacts more efficiently with all the positive centers of the cation. In contrast, in the liquid anions move toward a location along the C−H axis because in this way the electrostatic interactions with all the neighboring ions are optimized. Therefore, in the liquid the local minimum b) of Figure 2 seems to be stabilized with respect to the lower energy isomer a). This explains the shift in the position of the first peak in the two top panels of Figure 6 and also the differences observed in bond length, bond angle, and dihedral distributions between the gas and the liquid phase. The distances and angles in the liquid, however, are also quite different from those in the gas-phase isomer b), due to the presence of other $[DMIM]^+$ ions in the first solvation shell of the anions.

Figure 7 shows intermolecular hydrogen−hydrogen radial distribution functions. In general, all the functions are feature-

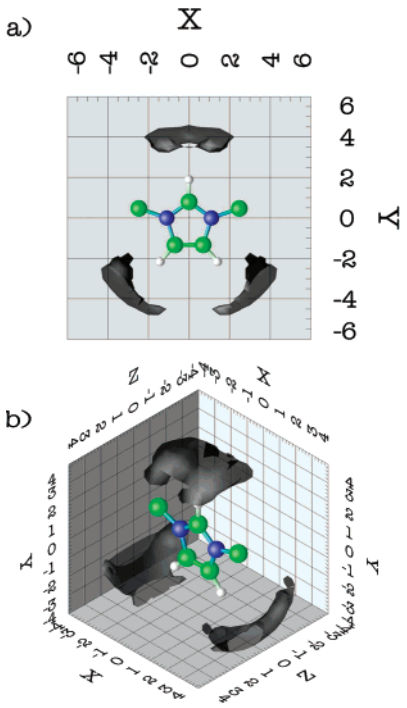

Figure 8. a − b: Probability distribution of Cl^- around $[DMIM]^+$. The isosurface corresponds to a density level of 0.03 $Å^{-3}$ which is 6 times the average number density of the chloride. Methyl-hydrogens have been omitted from the molecular model, for the sake of clarity.

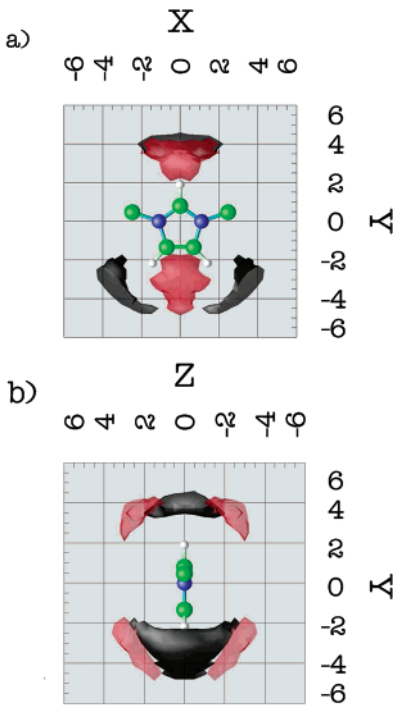

Figure 9. a − b: Superposition of probability distributions of both, anions (black) and ring-hydrogens (red). The density level of Cl^- is the same of Figure 8 while that for hydrogens is 0.025 $Å^{-3}$, which is 1.85 times their average number density. Methyl-hydrogens have been omitted from the molecular model, for the sake of clarity.

less. This is reasonable, because cations are separated by the first anion solvation shell. Only a strong cation orientational correlation could cause the hydrogen−hydrogen distributions to exhibit structure. Otherwise, the spherical average tends to erase any details.

As mentioned in section 3, cation−cation correlations are prone to statistical errors. Therefore, to calculate the quantities of Figure 7, in addition to the conventional average over different molecules, the equivalence between different atomic sites was also exploited. For the less abundant hydrogens, error bars are larger and a stronger dependence is observed with the size of the system. This effect is particularly noticeable in the H_2-H_2 distribution, but it also affects the $H_{4,5}-H_2$ and $H_{4,5}-H_{4,5}$ curves. In contrast, distribution functions involving methyl-hydrogens are very well converged and do not exhibit any size effects.

The lack of structural features in Figure 7 is, in some cases, at odds with the experiment. There, weak features were observed between methyl-hydrogens themselves and between methyl-hydrogens and H_8. It has to be remarked that classical simulations with different force fields, and for integration times of the order of nanoseconds, showed curves similar to the ab initio results discussed above. Therefore, the discrepancy cannot be attributed to insufficient statistical sampling, and we believe it may be due to difficulties in the interpretation of experimental data.

Being functions of a single variable, site−site distributions are easy to visualize and to interpret. However, they can hide details contained in the full, angular-dependent pair density function. Figure 8a and 8b show the spatial distribution of anions around a central cation, $\Omega_{Cl}(r,\theta,\phi)$. The C_{2v} symmetry of the cation was used to symmetrize $\Omega_{Cl}(r,\theta,\phi)$. The isosurface plotted corresponds to a density of 0.03 $Å^{-3}$ which is 6 times the average density of anions. There are three regions where the probability of finding a Cl^- is significantly large. These are associated with each one of the three ring C−H bonds. The highest density lobe corresponds to the anion located above the unique hydrogen H_8 and is visible even at 10 times the average density. Unlike the experiment, and in agreement with classical simulation, no density is observed above and below the plane of the ring even at very low probability levels.

In addition, anions are also concentrated in the vicinity of H_9 and H_{10}. In this case the contour surfaces are less symmetric with respect to the axis of the C−H bond, and the preferred position of the Cl^- moves toward the methyl-hydrogens, which carry a slightly positive charge. Only at very low probability levels anions are observed in positions axial to the methyl groups.

Taking into account the hydrogen coordination numbers reported before, we can conclude that the anion density lobes in Figure 8a and 8b correspond to a single anion associated with each ring-hydrogen. In turn, each of these anions is shared by three ring-hydrogens on different cations, all located at distances smaller than 3.5 Å.

Similar distributions have been published for a classical model[11] and for neutron experiments.[9,10] There are interesting differences between the present ab initio $\Omega_{Cl}(r,\theta,\phi)$ and those obtained from classical simulations. Classical force fields seem to systematically generate densities between the C−H bonds, while ab initio results indicate a high probability region above the ring hydrogens. This suggests a directionality in the H···Cl^- interaction of quantum mechanical origin, which classical point charge models fail to reproduce. This will be further explored in Section 4.4, but here it is worth mentioning that a possible improvement of classical force fields to enhance directionality could be to include local dipoles on the ring hydrogens, in the spirit of distributed multipole models.[32]

To understand better the organization of the liquid, in Figure 9a and 9b we show a superposition of the former anion density

and an isosurface of the ring-hydrogens (H_8, H_9, and H_{10}) probability density, $\Omega_H(r,\theta,\phi)$. This function gives the probability of finding an H_8, H_9, or H_{10} atom in a certain region around another $[DMIM]^+$ independently of the position of any other atom. The contour level plotted in the figures is 0.025 $Å^{-3}$ which is 1.85 times the average density of ring-hydrogens. Two regions can be distinguished, one around the anion density lobe, on top of the C_2-H_8 bond, and the other between the chlorides associated to H_9 and H_{10}. The lateral view in Figure 9b shows that each of these regions consists of two separated volumes, one above and another below the molecular plane. Such arrangement of hydrogens is consistent with the coordination numbers of Cl^- but is not accounted for in the H−H distributions of Figure 7. In this case the spherical average washes away a large amount of information. However, the charge ordering effect manifested by $\Omega_H(r,\theta,\phi)$ is reasonable and consistent with the charge ordering observed in other Ionic Liquids.[20]

The experimental results of Hardacre et al. have been frequently mentioned.[9,10] Therefore, a final comment is in order about the way in which spatial density functions and site−site distributions are extracted from neutron diffraction experiments. Given a set of diffraction data (structure factors) and a number of known constraints, the refinement algorithm (EPSR) generates an interatomic potential energy function that, through a Monte Carlo simulation, gives the best estimate of the measured structure factors. Although this procedure has been successfully applied to some molecular liquids,[23,24] its limitations in the study of complex binary fluids are less well-known. In the case of [DMIM][Cl], the total radial distribution functions does not contain enough information about intermolecular distances, while these are precisely the quantities used as target by the EPSR method. Therefore, similarities and differences between calculated and not directly measured structural properties must be treated with caution.

4.4. Hydrogen Bonding. Hydrogen bonds (H-bonds) are commonly accepted in chemistry as distinct interactions. However, its very definition is somewhat arbitrary. Depending on the definition adopted, interactions that span a wide range of energies can be classified as H-bonds.[33,34] In the most general case, H-bonds are directional interactions that occur whenever a hydrogen atom, bonded to an electronegative element, is close to a negatively charged center. In such an environment the hydrogen is attracted by two atoms rather than one.

The nature of the hydrogen bond is mainly electrostatic, although some degree of charge transfer and other quantum effects can contribute significantly, thereby making the interaction partially covalent.[33,34] This is the case, for example, for very strong H-bonds, such as those involved in certain intramolecular keto−enol equilibria,[33] where a large charge-transfer contribution is always present. Geometric, energetic and spectroscopic criteria have been used to classify them into strong, moderate and weak, but the limits between such categories are, of course, diffuse.[34]

Nowadays it seems quite well accepted that hydrogen bonding influences the structure of Ionic Liquids to an extent determined by the acceptor ability of the anion.[9,10] The aim of this section is to discern, using simple geometric criteria, to what extent the chloride-hydrogen contacts observed in the liquid phase can be considered as H-bonds.

To visualize the distribution of Cl^- in the vicinity of the C−H groups, a cylindrical average around the bond axis was constructed. This axis defined the Z direction, and the origin of the coordinate system was located at the hydrogen atom. Only hydrogens attached to the ring were considered. Figure 10a and 10b show the average density of Cl^- in any plane containing the C−H bond, relative to a uniform distribution. As indicated by site−site distributions (Figure 6), anions are localized 2.2 Å away from the hydrogens. More importantly, the shorter the contact the more linear the geometry of the C−*H*···Cl^- bond. This occurs because ring-hydrogens are partially deshielded thus giving rise to a dipole moment along the C−H bond.

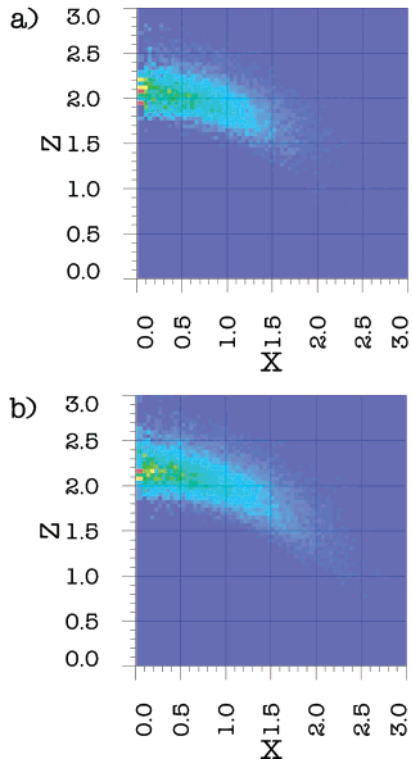

Figure 10. a − b: Chloride probability distribution around (a) the C_2-H_8 and (b) the $C_{4,5}-H_{9,10}$ bonds. The figures show the cylindrically averaged density around the C−H bond axis, relative to a random distribution. The direction Z coincides with the C−H bond, and the origin is located on the hydrogen atom.

Based on the criteria proposed by Jeffrey,[34] this kind of contact can be classified as a moderate hydrogen bond, since the C−H distance (1.1 Å) is much shorter than the H···Cl^- distance (2.2 Å) and the average angles for $C_2-H_8\cdots Cl^-$ and $C_{4,5}-H_{9,10}\cdots Cl^-$ are 151° and 148° respectively. Apart from directionality criteria, also the frequencies of the stretching modes of C_2-H_8 and $C_{4,5}-H_{9,10}$ in the liquid are red-shifted by 11% and 9% with respect to those in the isolated $[DMIM]^+$. That shift was estimated from the time-series of the C−H distances, both in the liquid phase and in the isolated cation.

Chemical intuition suggests that hydrogen-chloride interactions are attractive and can thus determine the structure of the first coordination shell of both ions. However, this reasoning can only be partially true. Interatomic distances in liquids result from a balance of all the interatomic forces and are not univocally related to a single interaction. In fact, distances in the most stable configuration of the isolated ion pair are quite different from those in the liquid phase, even when hydrogen-chloride interactions are also present. Directional interactions in the gas phase are already associated with higher energy isomers. However, it is only in the condensed phase, where ions are shared by several neighbors, that the anions spontaneously displace to the perimeter of the ring and recover the directionality in the H···Cl^- contacts.

5. Conclusions

We have carried out extensive ab initio simulations of the ionic liquid 1,3-dimethylimidazolium chloride. The structure of the liquid phase was described by several sets of site−site radial distributions, as well as three-dimensional density functions. The results are in very good agreement with recent neutron diffraction experiments.

The structure of the first solvation shell of $[DMIM]^+$ is characterized by a set of Cl^- ions localized in the neighborhood of ring-hydrogens. The contacts are quite directional due to the dipole moment associated with the C−H bond. In addition to directionality, the red shift in the stretching frequencies of the C_2-H_8 and $C_{4,5}-H_{9,10}$ bonds suggest an interpretation of these interactions as moderate hydrogen-bonds.

Short-range order in the liquid is reminiscent of that in the solid phase. Intermolecular hydrogen−hydrogen distributions show virtually no structure at the level of radial distances. However, the space distribution of H_8, H_9 and H_{10} around a central cation reveals regions where the local density is higher than the average. The comparison of anion and ring-hydrogen 3D-distributions indicates an arrangement of alternating charges, when observed from the local frame of $[DMIM]^+$. This charge alternation suggests a very efficient screening mechanism in Ionic Liquids, probably indicating a rather short screening length,[20] of the order of one or two solvation shells.

The calculated structural descriptors of cation−anion distances are well converged with respect to system size and to the time scales of the simulations. This shows that it is possible to use purely ab initio simulations to study structural features of Ionic Liquids. However, the use of classical simulations to generate uncorrelated initial configurations is extremely important. In addition, the results presented in this work can be used as a guideline and benchmark in the construction and subsequent validation of classical force fields for Ionic Liquids. One possible improvement would be to include local dipole moments on the ring hydrogens in addition to point charges. This would make cation−anion interactions more directional and thus more realistic.

The changes observed in the cation−anion distributions between the gas and liquid phases put a note of caution in the use of gas-phase ab initio calculations to rationalize structural and energetic properties of Ionic Liquids, or even to parametrize intermolecular interactions.

Acknowledgment. This work was funded by EPSRC, grant GR/S41562. R.M.L.B. thanks the Leverhulm Trust for an Emeritus Fellowship. Technical support by C. Sánchez and fruitful discussions with C. Hardacre, C. Pinilla and T. Youngs are acknowledged. We also thank C. Hardacre for providing and authorizing us to reproduce the experimental data reported in Figure 4.

Supporting Information Available: All the site−site pair distribution functions for the system of 8 ion-pairs reported in this paper are made available for use of those developing classical force fields. This material is available free of charge via the Internet at http://pubs.acs.org.

References and Notes

(1) Rogers, R. D.; Seddon, K. R.; Volkov, S. *Green Industrial Applications of Ionic Liquids;* NATO Science Series, 2002.
(2) Wasserscheid, P., Welton, T., Eds.; *Ionic Liquids in Synthesis;* Wiley VCH: 2002.
(3) Ingram, J. A.; Moog, R. S.; Ito, N.; Biswas, R.; Maroncelli, M. *J. Phys. Chem. B* **2003**, *107*, 5926−5932.
(4) Giraud, G.; Gordon, C. M.; Dunkin, I. R.; Wynne, K. *J. Chem. Phys.* **2003**, *119*, 464−477.
(5) Triolo, A.; Russina, O.; Arrighi, V.; Juranyi, F.; Janssen, S.; Gordon, C. M. *J. Chem. Phys.* **2003**, *119*, 8549−8557.
(6) Cavalcante, A. O.; Ribeiro, M. C. C. *J. Chem. Phys.* **2003**, *119*, 8567−8576.
(7) Lee, K. M.; Chang, H.-C.; Jiang, J.-C.; Lu, L.-C.; Hsiao, C.-J.; Lee, Y.-T.; Lin, S. H.; Lin, I. J. B. *J. Chem. Phys.* **2004**, *120*, 8645−8650.
(8) Xu, W.; Cooper, E. I.; Angell, C. A. *J. Phys. Chem. B* **2003**, *107*, 6170−6178.
(9) Hardacre, C.; Holbrey, J. D.; McMath, S. E. J.; Bowron, D. T.; Soper, A. K. *J. Chem. Phys.* **2003**, *118*, 273−278.
(10) Hardacre, C.; McMath, S. E. J.; Nieuwenhuyzen, M.; Bowron, D. T.; Soper, A. K. *J. Phys.: Condens. Matter* **2003**, *15*, S159−S166.
(11) Hanke, C. G.; Price, S. L.; Lynden-Bell, R. M. *Mol. Phys.* **2001**, *99*, 801−809.
(12) de Andrade, J.; Boes, E.; Stassen, H. *J. Phys. Chem. B* **2002**, *106*, 3546−3548.
(13) de Andrade, J.; Boes, E.; Stassen, H. *J. Phys. Chem. B* **2002**, *106*, 13344−13351.
(14) Urahata, S. M.; Ribeiro, M. C. C. *J. Chem. Phys.* **2004**, *120*, 1855−1863.
(15) Margulis, C.; Stern, H.; Berne, B. *J. Phys. Chem. B* **2002**, *106*, 12017−12021.
(16) Lopes, J. N. C.; Deschamps, J.; Padua, A. A. H. *J. Phys. Chem. B* **2004**, *108*, 2038.
(17) Yan, T.; Burnham, C. J.; Del Pópolo, M. G.; Voth, G. A. *J. Phys. Chem. B* **2004**, *108*, 11877−11881.
(18) Shah, J.; Brennecke, J.; Maginn, E. *Green Chem.* **2002**, *4*, 112−118.
(19) Lynden-Bell, R. M.; Atamas, N. A.; Vasilyuk, A.; Hanke, C. G. *Mol. Phys.* **2002**, *100*, 3225−3229.
(20) Del Pópolo, M. G.; Voth, G. A. *J. Phys. Chem. B* **2004**, *108*, 1744−1752.
(21) Hanke, C. G.; Atamas, N. A.; Lynden-Bell, R. M. *Green Chem.* **2002**, *4*, 107−111.
(22) Turner, E. A.; Pye, C. C.; Singer, R. D. *J. Phys. Chem. A* **2003**, *107*, 2277−2288.
(23) Soper, A. K. *Chem. Phys.* **1996**, *202*, 295−306.
(24) Soper, A. K. *Mol. Phys.* **2001**, *99*, 1503−1516.
(25) Soler, J. M.; Artacho, E.; Gale, J.; García, A.; Junquera, J.; Ordejón, P.; Sánchez-Portal, D. *J. Phys.: Condens. Matter* **2002**, *14*, 2745−2779.
(26) Perdew, J. P.; Burke, K.; Ernzerhof, M. *Phys. Rev. Lett.* **1996**, *77*, 3865−3868.
(27) Troullier, N.; Martins, J. L. *Phys. Rev. B* **1991** *43*, 1993.
(28) Hutter, J.; Parrinello, M. *Car-Parrinello Code (CPMD) developed by J. Hutter et al. at IBM Zurich Research Laboratory and the group of M. Parrinello at MPI, Stuttgart;* Copyright IBM Corp 1990−2004, Copyright MPI fur Festkrperforschung Stuttgart 1997−2001, 2004.
(29) Fannin, A. A.; King, L. A.; Levisky, J. A.; Wilkes, J. S. *J. Phys. Chem.* **1984**, *88*, 2609−2614.
(30) Arduengo, A. J.; Dias, H. V. R.; Harlow, R. L.; Kline, M. *J. Am. Chem. Soc.* **1992**, *114*, 5530−5534.
(31) Hansen, J.-P.; McDonald, I. R. *The Theory of Simple Liquids;* Academic Press: 1986.
(32) Willock, D. J.; Price, S. L.; Leslie, M.; Catlow, C. R. A. *J. Comput. Chem.* **1995**, *16*, 628−647.
(33) Desiraju, G. R. *Acc. Chem. Res.* **2002**, *35*, 565−573.
(34) Jeffrey, G. A. *An Introduction to Hydrogen Bonding;* Oxford University Press: 1997.